



HAL
open science

Half-sandwich Mo(III) complexes with asymmetric diazadiene ligands

François Stoffelbach, Philippe Richard, Rinaldo Poli, Titus Jenny, Corinne Savary

► **To cite this version:**

François Stoffelbach, Philippe Richard, Rinaldo Poli, Titus Jenny, Corinne Savary. Half-sandwich Mo(III) complexes with asymmetric diazadiene ligands. *Inorganica Chimica Acta*, 2006, 359 (14), pp.4447-4453. 10.1016/j.ica.2006.04.013 . hal-03195897

HAL Id: hal-03195897

<https://hal.science/hal-03195897>

Submitted on 12 Apr 2021

HAL is a multi-disciplinary open access archive for the deposit and dissemination of scientific research documents, whether they are published or not. The documents may come from teaching and research institutions in France or abroad, or from public or private research centers.

L'archive ouverte pluridisciplinaire **HAL**, est destinée au dépôt et à la diffusion de documents scientifiques de niveau recherche, publiés ou non, émanant des établissements d'enseignement et de recherche français ou étrangers, des laboratoires publics ou privés.

Half-sandwich Mo(III) complexes with asymmetric diazadiene ligands

François Stoffelbach,^a Philippe Richard,^a Rinaldo Poli^{*b}, Titus Jenny^c and Corinne Savary^c

^a*Laboratoire de Synthèse et d'Electrosynthèse Organométalliques, UMR-CNRS-5188, Faculté des Sciences "Mirande", Université de Bourgogne, 9 Avenue Alain Savary, 21078 Dijon CEDEX, France*

^b*Laboratoire de Chimie de Coordination, UPR CNRS 8241, lié par convention à l'Université Paul Sabatier et à l'Institut National Polytechnique de Toulouse, 205 Route de Narbonne, 31077 Toulouse Cedex, France.*

^c*Département de Chimie, Université de Fribourg, Route du Musée 9, CH-1700 Fribourg, Switzerland*

Proofs to:

Rinaldo Poli

Tel: +33-561333195

Fax: +33-561553003

E-mail: poli@lcc-toulouse.fr

Summary

The asymmetric 1,4-diazadiene ligands $R^*N=CHCH=NR^*$ [$R^* = (S)\text{-CH}(\text{CH}_3)\text{Ph}$], **R*₂dad**, and 2,2'-bis(4-ethyloxazoline), **as-ox**, have been used to generate half-sandwich Mo^{III} derivatives by addition to $\text{Cp}_2\text{Mo}_2\text{Cl}_4$. Ligand **R*₂dad** affords a mononuclear, paramagnetic 17-electron product, $\text{CpMoCl}_2(\text{R}^*\text{₂dad})$, whereas **as-ox** leads to the isolation of a dinuclear compound where only one molecule of ligand has been added per two Mo atoms, $\text{Cp}_2\text{Mo}_2\text{Cl}_4(\text{as-ox})$. In the presence of free **as-ox**, this compound coexists with the paramagnetic mononuclear complex in solution. Both products are capable to control the radical polymerization of styrene under typical atom transfer radical polymerization (ATRP) conditions. However, the tacticity of the resulting polystyrene does not differ from that given by conventional free radical polymerization.

Keywords

Molybdenum, Atom Transfer Radical Polymerization, Polystyrene, Half-sandwich Complexes, Diazadiene

Introduction

In recent years, a number of coordination and organometallic compounds based on different transition metals have been shown to be capable of controlling the radical polymerization of activated olefins through a process that has been termed Atom Transfer Radical Polymerization (ATRP), see Scheme 1.^[1, 2] The active radical concentration is maintained at very low levels through a reversible equilibrium with a dormant species, thereby reducing the incidence of bimolecular terminations.

<Scheme 1>

Systems based on a variety of transition metals, including Ti^{III} ,^[3] Mo^{III} ,^[4, 5] Re^V ,^[6] Fe^{II} ,^[7, 8] Ru^{II} ,^[9] Ni^{II} ,^[10] Ni^0 ,^[11] and Cu^I ,^[12] have been shown effective. Although no system currently appears to parallel the activities and practical advantages of certain Cu^I complexes, the investigation of other metal systems is useful in order to shine light on the mechanistic details of the process.

In spite of many observations in agreement with the mechanism shown in Scheme 1, certain experimental facts have suggested the possibility of a more complex mechanism. For instance, it has been shown that a large amount of phenol does not inhibit the ATRP of MMA catalyzed by copper(I) bromide,^[13] and that the medium polarity could have an important effect on the rate of polymerization.^[14, 15] Recently, a different ^{13}C isotope effect has been reported for the Cu^I -catalyzed ATRP of methyl methacrylate relative to the free radical polymerization process, suggesting a difference in the nature of the transition state for the propagation step.^[16] Although these data have later been fully rationalized without the need to modify the mechanism,^[17] further work has shown that, under certain circumstances and for

certain catalysts, the monomer can coordinate to the metal center.^[18] This feature seems to open the way to the growth of stereoregular polymers, provided the metal is contained within an asymmetric coordination environment, the olefin coordination step is enantioselective, and the coordinated monomer is more susceptible than the free monomer to radical addition. The control of stereochemistry in radical polymerization attracts considerable interest. Moderate success in this goal has been achieved by using a grafted chiral auxiliary on the monomer^[19] and by using a Lewis acid additive which is capable to reversibly interact with the monomer.^[20, 21]

Since we have recently developed a series of active ATRP catalysts based on half-sandwich molybdenum complexes of 1,4-diazadiene ligands,^[5, 22, 23] and since asymmetric versions of such ligands are well established,^[24] we have decided to prepare the related Mo complexes and to test them in controlled radical polymerization.

Experimental Section

General procedures. (a) Materials. All manipulations were carried out under an atmosphere of dry and oxygen-free argon with standard Schlenk techniques. Toluene, THF and pentane were purified by reflux over sodium benzophenone ketyl and distilled under argon prior to use. CH₂Cl₂ was dehydrated with P₄O₁₀ and distilled under argon. Styrene was washed with an aqueous NaOH solution (10%), followed by water, then dried over MgSO₄ and finally distilled at 25°C under reduced pressure. (1-Bromoethyl)benzene (BEB) and Al(O-*i*-Pr)₃ (Aldrich) were used as received. [CpMo(μ-Cl)₂]₂^[25] and CH₃CH(I)COOEt (IEA)^[26] were prepared as described in the literature. Glyoxal (40% in water) and (*S*)-H₂NCH(CH₃)Ph (Aldrich) were used as received. The bisoxazoline ligands were prepared by

adapting and optimizing a known procedure^[27] involving commercial chiral aminoalcohols (Fluka).

(b) Physical measurements. Molecular weights and molecular weight distributions were measured with a Gynkoteck P580 size exclusion chromatographer equipped with a refractometer and 2 B Jordi DVB columns (range 1000-1000000) using THF as eluent (1mL/min). The instrument was calibrated by using polystyrene standards. EPR measurements were carried out at the X-band microwave frequency on a Bruker ESP300 spectrometer. The spectrometer frequency was calibrated with diphenylpicrylhydrazyl (DPPH, $g = 2.0037$). Cyclic voltammograms were recorded with an EG&G 362 potentiostat connected to a Macintosh computer through MacLab hardware/software. The electrochemical cell was fitted with an Ag-AgCl reference electrode, a platinum disk working electrode and a platinum wire counter-electrode. $[\text{Bu}_4\text{N}]\text{PF}_6$ (ca. 0.1 M) was used as supporting electrolyte in THF. All potentials are reported relative to the ferrocene standard, which was added to each solution and measured at the end of the experiments. The elemental analyses were carried out by the analytical service of the LSEO laboratory with a Fisons EA 1108 apparatus. NMR spectra were recorded on a Bruker DRX 500 spectrometer. The peaks positions are reported with positive shifts in ppm downfield of TMS, as calculated from residual solvent peaks.

Preparation of R^*dad [$\text{R}^* = (S)\text{-CH}(\text{CH}_3)\text{Ph}$]. Glyoxal (0.9 g, 15.5 mmol) and $(S)\text{-PhCH}(\text{CH}_3)\text{NH}_2$ (4 mL, 31.0 mmol) were mixed in 10 mL of MeOH at room temperature. The mixture was then stirred for 3 h at 70°C. The ligand was extracted with 60 mL of heptane. An oil was obtained by cooling the solution to -80°C. After decanting off the mother liquor, the oil was distilled under reduced pressure. ^1H NMR (CDCl_3 , 25°C): δ 1.60 (d, $J = 6.7$ Hz, CH_3), δ 4.52 (q, $J = 6.7$ Hz, CH), δ 7.20-7.40 (m, Ph), δ 8.07 (s, $\text{CH}=\text{N}$).

Synthesis of complex $\text{CpMoCl}_2[\text{R}^*\text{dad}]$. $[\text{CpMo}(\mu\text{-Cl})_2]_2$ (0.360 g, 0.78 mmol) and R^*dad (0.183 g, 1.78 mmol) were suspended in 15 mL of toluene at room temperature. The

mixture was then stirred for 24 h at 70°C. The solution was filtered through Celite to remove a small amount of residual solid and concentrated under reduced pressure to ca. 6 mL. Addition of 10 mL of pentane gave the product as a red brown microcrystalline solid, which was washed with pentane (3 x 5 mL) and dried in vacuo. Yield: 0.502 g (65%). *Anal.* Calc. for C₂₃H₂₅Cl₂MoN₂: C 55.66, H 5.08, N 5.64 %. Found: C 55.05, H 5.53, N 5.16 %. EPR (CH₂Cl₂): g = 1.976 (a_{Mo} = 45.2 G). Cyclic voltammetry (THF): reversible oxidation with E_{1/2} = +0.05 V (ΔE_p = 81 mV) and reversible reduction at E_{1/2} = -1.04 V (ΔE_p = 76 mV). The ferrocene peak showed ΔE_p = 130 mV.

Synthesis of Cp₂Mo₂Cl₄(*as-ox*). [CpMo(μ-Cl)₂]₂ (0.557 g, 1.20 mmol) and *as-ox* (0.470 g, 2.39 mmol) were suspended in 15 mL of dichloromethane at room temperature. The mixture was then stirred for 4 h at RT. The blue solution was filtered through Celite to remove a small amount of residual solid and evaporated to dryness under reduced pressure. The dark microcrystalline solid was then washed with 7 mL of pentane and dried in vacuo. Yield: 0.453 g (57%). A recrystallization from CH₂Cl₂/pentane afforded X-ray quality crystals, one of which was used for the X-Ray structural study.

ATRP polymerizations. All ATRP polymerization reactions were performed following the same experimental procedure. The complex was added to a 50 mL Schlenk tube equipped with a stirring bar. Styrene and (1-bromoethyl)benzene were added to the reaction flask by a syringe. The Schlenk tube was then immersed in an oil bath heated at 90°C. Aliquots were withdrawn periodically for a reaction monitoring by GPC.

Single crystal X-ray diffraction study. Intensities were collected with a Nonius Kappa CCD diffractometer at 110 K. The structure was solved via a Patterson search program (DIRDIF-99)^[28] and refined with full-matrix least squares methods based on F² (SHELX-97)^[29] with the aid of the WINGX^[30] program. All non-hydrogen atoms were refined with anisotropic thermal parameters. All H atoms were placed in idealized positions and refined

using a riding model [$U_{iso}(H) = 1.2U_{eq}(C)$, 1.5 for methyl groups]. The essential crystallographic parameters are listed in Table 1 and selected bond distances and angles are collected in Table 2.

<Table 1 and Table 2 here>

Crystallographic data (excluding structure factors) have been deposited with the Cambridge Crystallographic Data Centre as supplementary publication no. CCDC 271075. Copies of the data can be obtained free of charge on application to the Director, CCDC, 12 Union Road, Cambridge CB2 1EZ, UK (fax: (+44) 1223-336-033; e-mail: deposit@ccdc.cam.ac.uk).

Results and Discussion

(a) Syntheses and characterization

The asymmetric (*S,S'*)- $R^*N=CHCH=NR^*$ [$R^* = CH(CH_3)Ph$] ligand (**R*₂dad**) has been prepared by following the same general procedure consisting of the double condensation between glyoxal and the suitable primary amine,^[31-34] see Scheme 2. The bisoxazoline ligands were prepared by reaction of the corresponding chiral aminoalcohols with ethyl oxalate to form the bis-amide, followed by substitution of the alcohol functions by chloride and subsequent ring closure to yield the chiral bisoxazolines (**as-ox**).^[27]

<Scheme 2>

The synthesis of complex $\text{CpMoCl}_2(\mathbf{R}^*\mathbf{2dad})$ has followed the same procedure that were previously reported for the related $\text{CpMoCl}_2(\text{R}_2\text{dad})$ complexes ($\text{R} = i\text{Pr}, \text{Ph}, p\text{-Tol}, \text{C}_6\text{H}_3i\text{Pr}_{2-2,6}$), see Scheme 3.^[5] The isolated product has been characterized by EPR spectrometry ($g = 1.976$ et $a_{\text{Mo}} = 45.2$ G) and by electrochemistry (reversible oxidation at $E_{1/2} = +0.05$ V and reversible reduction at $E_{1/2} = -1.04$ V, in THF). These properties are essentially identical to those previously reported for complex $\text{CpMoCl}_2(i\text{Pr}_2\text{dad})$ ($g = 1.975$; $a_{\text{Mo}} = 42.8$ G; $E_{1/2\text{ox}} = 0.01$ V; $E_{1/2\text{red}} = -1.10$ V), to which it is closely related in terms of steric and electronic properties.

<Scheme 3>

When an identical procedure was carried out using **as-ox**, the course of the reaction was visually quite different. Contrary to the reaction with $\mathbf{R}^*\mathbf{2dad}$, which gave a brown solution (like all other previously investigated R_2dad complexes, but also typical of all mononuclear $\text{CpMoCl}_2\text{L}_2$ complexes with $\text{L} = \text{phosphine}$ or $\text{L}_2 = \text{diphosphine}$ or diene), the reaction with **as-ox** gave a deep blue solution. The solution EPR spectrum is consistent with the presence of expected mononuclear $\text{CpMoCl}_2(\mathbf{as-ox})$ complex ($g = 2.006$, $a_{\text{Mo}} = 32.6$ G). However, crystallization by slow diffusion of pentane into the reaction mixture in dichloromethane yielded blue crystals, which were revealed to correspond to the dinuclear complex $\text{Cp}_2\text{Mo}_2\text{Cl}_4(\mathbf{as-ox})$ by a single crystal X-ray analysis (see Figure 1).

<Figure 1>

The geometry of the compound can be seen as two four-legged piano stools sharing two legs and is precedente for other dinuclear half-sandwich complexes of Mo(III), such as $[\text{Cp}_2\text{Mo}_2(\mu\text{-S}t\text{Bu})_2(\text{CO})_4]^{2+}$.^[35] However, this type of structure is unprecedented for neutral

derivatives of molybdenum(III), *i.e.* of type $\text{Cp}_2\text{Mo}_2\text{X}_4\text{L}_2$. The addition of neutral ligands to $\text{Cp}_2\text{Mo}_2\text{Cl}_4$ has previously been shown to give either mononuclear CpMoX_2L_2 -type compounds directly when the ligand has strong donor properties, or no reaction at all in the case of poor ligands (*e.g.* amines, ethers). Compound $\text{Cp}_2\text{Mo}_2\text{Cl}_4(\text{as-ox})$ can be viewed as an intermediate of the process converting the tetrachloro-bridged precursor to the mononuclear bis-ligand adduct. Therefore, the donor properties of the **as-ox** ligand are in the narrow grey area between those two regions. As the EPR spectrum suggests, the mononuclear compound probably exists in solution, though in equilibrium with the blue dinuclear complex, and it is the latter that crystallized preferentially, see Scheme 4. Because of this equilibrium, no informative NMR spectrum could be recorded for the dinuclear complex. A molecule structurally related to complex $\text{Cp}_2\text{Mo}_2\text{Cl}_4(\text{as-ox})$ has been reported for tungsten, $\text{Cp}'_2\text{W}_2\text{Cl}_4(\text{dmpe})$ ($\text{Cp}' = \text{C}_5\text{H}_4\text{Me}$; $\text{dmpe} = \text{Me}_2\text{PCH}_2\text{CH}_2\text{PMe}_2$).^[36] Interestingly, no mononuclear complex of type CpMX_2L_2 has been reported for W(III) to the best of our knowledge. The reason of the different behaviour between molybdenum and tungsten, for the outcome of the ligand addition to $[\text{CpMCl}_2]_2$ -type compounds, is related to the stronger metal-metal interactions established by the latter metal.^[37] For molybdenum, mononuclear CpMoX_2L_2 complexes are the rule and the dinuclear $\text{Cp}_2\text{Mo}_2\text{X}_4\text{L}_4$ -type complex reported here is the exception, whereas for tungsten even the strong dmpe ligand stops at the dinuclear $\text{Cp}_2\text{Mo}_2\text{X}_4\text{L}_4$ -type complex.

<Scheme 4>

The most interesting structural parameter of the $\text{Cp}_2\text{Mo}_2\text{Cl}_4(\text{as-ox})$ compound is the metal-metal distance [3.124(5) Å]. It is well known that the stepwise opening of the four bridges in $\text{Cp}_2\text{Mo}_2\text{Cl}_4$ is accompanied by a weakening of the metal-metal interaction. Indeed

this distance is shorter in the quadruply-bridged $\text{Cp}'_2\text{Mo}_2(\mu\text{-Cl})_4$ [2.607(1) Å]^[38] and $\text{Cp}_2\text{Mo}_2(\mu\text{-SMe})_4$ [2.603(2) Å],^[39] intermediate in triply bridged $[\text{Cp}_2\text{Mo}_2(\mu\text{-SMe})_3(\text{CO})_2]^+$ [2.785(2) Å]^[40] and $[\text{Cp}_2\text{Mo}_2(\mu\text{-SMe})_2(\mu\text{-SH})(\text{CO})_2]^+$ [2.772(2) Å],^[41] and longer in doubly bridged $[\text{Cp}_2\text{Mo}_2(\mu\text{-}i\text{tBu})_2(\text{CO})_4]^{2+}$ [3.008(2) Å],^[35] $[\text{Cp}_2\text{Mo}_2(\mu\text{-SMe})_2(\text{MeCN})_4]^{2+}$ [3.0000(6) Å]^[42] and $[\text{Cp}_2\text{Mo}_2(\mu\text{-SPh})_2(\text{CO})_3(\text{MeCN})]^+$ [3.006(3) Å].^[43] For the related W complex $\text{Cp}'_2\text{W}_2\text{Cl}_4(\text{dmpe})$, the W-W distance is 3.196(1) Å.^[36] Another interesting feature is the variation of the Mo-Cl bond distance and the bond distances related to the Mo(dad) moiety, in comparison with the structure of $\text{CpMoCl}_2[(\text{C}_6\text{H}_3i\text{Pr}_{2-2,6})_2\text{dad}]$.^[44] The terminal Mo(2)-Cl distances [average 2.48(2) Å] are much longer than in the mononuclear complex [average 2.40(2) Å], but correspond closely to those of other $\text{CpMoCl}_2\text{L}_2$ compounds (*e.g.* average of 2.471(3) Å^[45] for L = PMe_3). The bridging Mo-Cl bonds are also longer [average 2.45(1) Å]. On the other hand, the N-C and C-C distances of the bis(oxazoline) ligand are respectively shorter [average 1.284(7) Å] and longer [1.446(6) Å] than the same distances in the mononuclear complex [1.352(2) Å and 1.363(2) Å, respectively]. All these differences point to a more appropriate description of the coordination as involving a dative interaction between the neutral bis(oxazoline) ligand and a Mo^{III} center, whereas the mononuclear complex has a stronger contribution from a resonance form formally viewed as containing a covalently bonded (enediamido) Mo^{V} moiety. Other complexes where diazadiene ligands bind prevalently through a dative interaction also display shorter C-N and longer C-C distances, *e.g.* average 1.269(4) Å and 1.476(4) Å, respectively, in $\text{MoO}_2\text{Cl}_2(i\text{tBu}_2\text{dad})$.^[46] The Mo atom is close to the least squares plane defined by the N-C-C-N chelate (distance = 0.20(1) Å).

(b) Controlled radical polymerizations

Complexes $\text{CpMoCl}_2(\mathbf{R}^*\mathbf{2dad})$ and $\text{Cp}_2\text{Mo}_2\text{Cl}_4(\mathbf{as-ox})$ have been tested as catalysts for the ATRP of styrene. The polymerization with the former complex was carried out under the typical conditions already applied for related $\text{CpMoCl}_2(\mathbf{R}_2\text{dad})$ compounds, using the iodo derivative $\text{CH}_3\text{CH}(\text{I})\text{COOEt}$ (IEA) as an initiator, and one equivalent of $\text{Al}(\text{OiPr})_3$ as a co-catalyst.^[5] A rationalization for the mode of action of this co-catalyst has been reported separately.^[22, 47] The results are shown in Figure 2. The polymerization with complex $\text{Cp}_2\text{Mo}_2\text{Cl}_4(\mathbf{as-ox})$ was carried out with 1-bromoethylbenzene (BEB) as an initiator, and without the $\text{Al}(\text{OiPr})_3$ co-catalyst. Both the IEA and BEB initiators have been shown to lead to a controlled polymerization of styrene with other Mo-based catalysts.^[5] For both systems, we observe that the molecular weights increase linearly with conversion and that the polydispersity indexes (PDI) are relatively low (down to ca. 1.3). Note that the initiator efficiency factor is low in each case ($f = 0.6$). The same phenomenon occurs for the previously described $\text{CpMoCl}_2(\mathbf{R}_2\text{dad})$ catalysts.^[5] In addition, the monomer consumption follows in each case first order kinetics, see Figure 3. This is as expected for a controlled process. The rate of monomer consumption is quite a bit slower with complex $\text{Cp}_2\text{Mo}_2\text{Cl}_4(\mathbf{as-ox})$ [$k_{\text{app}} = 5.4 \cdot 10^{-5} \text{ min}^{-1}$] than with the mononuclear complex $\text{CpMoCl}_2(\mathbf{R}^*\mathbf{2dad})$ [$k_{\text{app}} = 4.2 \cdot 10^{-4} \text{ min}^{-1}$]. The latter is close to that measure previously by using complex $\text{CpMoCl}_2(\mathbf{iPr}_2\text{dad})$ under the same conditions ($k_{\text{app}} = 3.0 \cdot 10^{-4} \text{ min}^{-1}$). The lower activity of the dinuclear complex could at least in part be attributed to the absence of the $\text{Al}(\text{OiPr})_3$ co-catalyst, since an accelerating factor of ca. 17 has been observed in the presence of one equivalent of this compound for the related $\text{CpMoCl}_2(\mathbf{iPr}_2\text{dad})$ catalysts.^[5]

The product obtained from each procedure was analyzed by ^{13}C NMR, in order to see whether the ligand asymmetry had any effect on the polymer tacticity.^[48, 49] However, no notable difference could be detected, relative to a polymer obtained by free radical polymerization (AIBN initiator).

<Figure 2 and Figure 3>

Conclusions

The well established family of half-sandwich $\text{CpMoCl}_2(\text{R}_2\text{dad})$ complexes has been extended to asymmetric members, one containing a chiral auxiliary on the nitrogen atom, **R*₂dad** [$\text{R}^* = (S)\text{-CH}(\text{CH}_3)\text{Ph}$], the second one being based on a C_2 -symmetric bis(oxazoline) donor, **as-ox**. The latter is the first reported example of a bis(oxazoline) derivative for the half-sandwich CpMo^{III} system. However, while the use of **R*₂dad** leads to the splitting of the dinuclear $\text{Cp}_2\text{Mo}_2\text{Cl}_4$ precursor, the **as-ox** ligand allows for the first time the isolation of a dinuclear adduct, which may be viewed as an intermediate of the dimer splitting process. Indeed, EPR spectroscopy indicates the presence of the mononuclear species in solution. Both complexes, like the previously investigated symmetric analogues, are capable to catalyze the atom transfer radical polymerization of styrene. However, there is no indication that the asymmetric nature of the catalyst exerts any stereocontrol in the polymerization process. Among other possible factors, the probable lack of coordination of the monomer to the asymmetric catalyst may contribute to this result. In fact, the 17-electron nature of the half-sandwich Mo^{III} center does not leave available positions for coordination of a 2-electron donor. It does, however, allow the increase of both the number of valence electrons and the coordination number by one unit, as required by the atom transfer process.

Acknowledgements. We are grateful to the CNRS for financial help. This project started with funding by a national CNRS program entitled “Catalyse et catalyseurs pour l’industrie et

l'environnement" (1997-98). The European COST D17 programme (working group D17/0007/00) is also acknowledged for additional financial help.

References

- [1] K. Matyjaszewski, J. H. Xia, *Chem. Rev.* **2001**, *101*, 2921.
- [2] M. Kamigaito, T. Ando, M. Sawamoto, *Chem. Rev.* **2001**, *101*, 3689.
- [3] Y. Kabachii, S. Kochev, L. Bronstein, I. Blagodatskikh, P. Valetsky, *Polym. Bull.* **2003**, *50*, 271.
- [4] E. Le Grogne, J. Claverie, R. Poli, *J. Am. Chem. Soc.* **2001**, *123*, 9513.
- [5] F. Stoffelbach, D. M. Haddleton, R. Poli, *Eur. Polym. J.* **2003**, *39*, 2099.
- [6] Y. Kotani, M. Kamigaito, M. Sawamoto, *Macromolecules* **1999**, *32*, 2420.
- [7] Y. Kotani, M. Kamigaito, M. Sawamoto, *Macromolecules* **1999**, *32*, 6877.
- [8] V. C. Gibson, R. K. O'Reilly, W. Reed, D. F. Wass, A. J. P. White, D. J. Williams, *Chem. Commun.* **2002**, 1850.
- [9] T. Ando, M. Kamigaito, M. Sawamoto, *Macromolecules* **2000**, *33*, 6732.
- [10] H. Uegaki, Y. Kotani, M. Kamigaito, M. Sawamoto, *Macromolecules* **1997**, *30*, 2249.
- [11] H. Uegaki, M. Kamigaito, M. Sawamoto, *J. Polym. Sci., Polym. Chem.* **1999**, *37*, 3003.
- [12] J. Guo, Z. Han, P. Wu, *J. Mol. Catal. A* **2000**, *159*, 77.
- [13] D. M. Haddleton, A. J. Clark, M. C. Crossman, D. J. Duncalf, A. M. Heming, S. R. Morsley, A. J. Shooter, *Chem. Commun.* **1997**, 1173.
- [14] D. M. Haddleton, S. Perrier, S. A. F. Bon, *Macromolecules* **2000**, *33*, 8246.
- [15] X. S. Wang, S. P. Armes, *Macromolecules* **2000**, *33*, 6640.
- [16] S. Harisson, J. Rourke, D. Haddleton, *Chem. Commun.* **2002**, 1470.
- [17] D. Singleton, D. Nowlan, N. Jahed, K. Matyjaszewski, *Macromolecules* **2003**, *36*, 8609.
- [18] W. A. Braunecker, T. Pintauer, N. V. Tsarevsky, G. Kickelbick, K. Matyjaszewski, *J. Organomet. Chem.* **2005**, *690*, 916.
- [19] N. A. Porter, B. Giese, D. P. Curran, *Acc. Chem. Res.* **1991**, *24*, 296.
- [20] Y. Isobe, Y. Suito, S. Habaue, Y. Okamoto, *J. Polym. Sci., Polym. Chem.* **2003**, *41*, 1027.
- [21] J. Lutz, D. Neugebauer, K. Matyjaszewski, *J. Am. Chem. Soc.* **2003**, *125*, 6986.
- [22] F. Stoffelbach, R. Poli, *Chem. Commun.* **2004**, 2666
- [23] R. Poli, F. Stoffelbach, S. Maria, J. Mata, *Chem. Eur. J.* **2005**, *11*, 2537.
- [24] H. Brunner, W. Zettelmeier, *Handbook of Enantioselective Catalysis, vol. II*, VCH, **1993**.
- [25] F. Abugideiri, R. Poli, in *Synthetic Methods of Organometallic and Inorganic Chemistry (Herrmann/Brauer), Vol. 8* (Ed.: W. A. Herrmann), Georg Thieme Verlag, Stuttgart, **1997**, pp. 102.
- [26] D. P. Curran, E. Bosch, J. Kaplan, M. Newcomb, *J. Org. Chem.* **1989**, *54*, 1826.
- [27] I. Butula, G. Karlovic, *Justus Liebigs Annalen der Chemie* **1976**, 1455.
- [28] P. T. Beurskens, G. Beurskens, R. d. Gelder, S. Garcia-Granda, R. Israel, R. O. Gould, J. M. M. Smits, *The DIRDIF-99 program system*, Crystallography Laboratory, University of Nijmegen, The Netherlands, **1999**.
- [29] G. M. Sheldrick, *SHELXL97. Program for Crystal Structure refinement*, University of Göttingen, Göttingen, Germany, **1997**.

- [30] L. J. Farrugia, *J. Appl. Crystallogr.* **1999**, *32*, 837.
- [31] J. M. Kliegman, R. K. Barnes, *J. Org. Chem.* **1970**, *35*, 3140.
- [32] J. M. Kliegman, R. K. Barnes, *Tetrahedron* **1970**, *26*, 2555.
- [33] H. tom Dieck, I. W. Renk, *Chem. Ber.* **1971**, *104*, 92.
- [34] L. Jafarpour, E. D. Stevens, S. P. Nolan, *J. Organomet. Chem.* **2000**, *606*, 49.
- [35] J. Courtot-Coupez, M. Guéguen, J. E. Guerchais, F. Y. Pétillon, J. Talarmin, R. Mercier, *J. Organometal. Chem.* **1986**, *312*, 81.
- [36] M. L. H. Green, P. Mountford, *J. Chem. Soc., Chem. Commun.* **1989**, 732.
- [37] M. L. H. Green, P. Mountford, *Chem. Soc. Rev.* **1992**, 29.
- [38] P. D. Grebenik, M. L. H. Green, A. Izquierdo, V. S. B. Mtetwa, K. Prout, *J. Chem. Soc., Dalton Trans.* **1987**, 9.
- [39] N. G. Connelly, L. F. Dahl, *J. Am. Chem. Soc.* **1970**, *92*, 7470.
- [40] M. B. Gomes de Lima, J. E. Guerchais, R. Mercier, F. Y. Pétillon, *Organometallics* **1986**, *5*, 1952.
- [41] P. Schollhammer, F. Y. Pétillon, R. Pichon, S. Poder-Guillou, J. Talarmin, K. W. Muir, L. Manojlovic-Muir, *Organometallics* **1995**, *14*, 2277.
- [42] P. Schollhammer, F. Y. Pétillon, J. Talarmin, K. W. Muir, *Inorg. Chim. Acta* **1999**, *284*, 107.
- [43] M. El Khalifa, M. Guéguen, R. Mercier, F. Y. Pétillon, J.-Y. Saillard, J. Talarmin, *Organometallics* **1989**, *8*, 140.
- [44] F. Stoffelbach, R. Poli, P. Richard, *J. Organometal. Chem.* **2002**, *663*, 269.
- [45] S. T. Krueger, R. Poli, A. L. Rheingold, D. L. Staley, *Inorg. Chem.* **1989**, *28*, 4599.
- [46] K. Dreisch, C. Andersson, C. Stalhandske, *Polyhedron* **1993**, *12*, 303.
- [47] R. Poli, F. Stoffelbach, S. Maria, J. Mata, *Chem. Eur. J.* **in press**.
- [48] Y. Inoue, A. Nishioka, R. Chujo, *Makromol. Chem.* **1972**, *156*, 207.
- [49] D. Baudry-Barbier, E. Camus, A. Dormond, M. Visseaux, *Appl. Organometal. Chem.* **1999**, *13*, 813.

Table 1. Crystal data and structure refinement for compound $\text{Cp}_2\text{Mo}_2\text{Cl}_4(\text{as-ox})$.

Formula	$\text{C}_{20}\text{H}_{26}\text{N}_2\text{O}_2\text{Cl}_4\text{Mo}_2$
M	660.11
T; K	110(2)
Crystal system	Orthorhombic
Space group	$P2_12_12_1$
a; Å	12.4051(6)
b; Å	13.6827(7)
c; Å	14.0961(8)
V; Å ³	2392.6(2)
Z	4
F(000)	1312
D _{calc} ; g/cm ³	1.833
diffractometer	Enraf-Nonius KappaCCD
scan type	mixture of ϕ rotations and ω scans
λ ; Å	0.71073
μ ; mm ⁻¹	1.515
Crystal size; mm ³	0.23 x 0.14 x 0.14
$\sin(\theta)/\lambda$ max; Å ⁻¹	0.65
Index ranges	h: -16 ; 12 k: -11 ; 17 l: -17 ; 18
RC = Refl. Collected	9714
IRC = independent RC	5226 [R(int) = 0.0499]
IRCGT = IRC and [I>2 σ (I)]	4094
Refinement method	Full-matrix least-squares on F ²
Data / restraints / parameters	5226 / 0 / 272
Absolute structure parameter	0.00(6)
R for IRCGT	$R1^a = 0.0415$, $wR2^b = 0.0683$
R for IRC	$R1^a = 0.0643$, $wR2^b = 0.0756$
Goodness-of-fit ^c	0.993
Largest diff. peak and hole; e.Å ⁻³	0.737 and -0.965

$$^a R1 = \frac{\sum(|F_o| - |F_c|)}{\sum|F_o|}$$

$$^b wR2 = \frac{[\sum w(F_o^2 - F_c^2)^2 / \sum [w(F_o^2)^2]^{1/2}}{\text{where } w = 1 / [\sigma^2(F_o^2) + (0.0184 * P)^2]} \text{ where } P = (\text{Max}(F_o^2, 0) + 2 * F_c^2) / 3$$

$$^c \text{Goodness of fit} = [\sum w(F_o^2 - F_c^2)^2 / (N_o - N_v)]^{1/2}$$

Table 2. Selected bond lengths [\AA] and angles [$^\circ$] for compound $\text{Cp}_2\text{Mo}_2\text{Cl}_4$ (*as*-dioxazoline).

Distances (\AA)			
Mo(1)-CNT(1)	1.949(6)	Mo(2)-CNT(2)	1.954(6)
Mo(1)-Cl(1)	2.4609(15)	Mo(2)-Cl(1)	2.4484(15)
Mo(1)-Cl(2)	2.4404(15)	Mo(2)-Cl(2)	2.4419(16)
Mo(1)-Cl(3)	2.4721(15)	Mo(2)-N(1)	2.148(5)
Mo(1)-Cl(4)	2.4774(16)	Mo(2)-N(2)	2.136(5)
Mo(1)-Mo(2)	3.1243(5)	C(8)-C(9)	1.446(6)
N(1)-C(8)	1.288(7)	N(2)-C(9)	1.280(7)

Angles ($^\circ$)			
CNT(1)-Mo(1)-Cl(1)	111.5(2)	CNT(2)-Mo(2)-Cl(1)	113.9(2)
CNT(1)-Mo(1)-Cl(2)	110.4(2)	CNT(2)-Mo(2)-Cl(2)	112.9(2)
CNT(1)-Mo(1)-Cl(3)	107.8(2)	CNT(2)-Mo(2)-N(1)	110.4(2)
CNT(1)-Mo(1)-Cl(4)	108.2(2)	CNT(2)-Mo(2)-N(2)	113.4(2)
Cl(1)-Mo(1)-Cl(2)	79.57(4)	Cl(1)-Mo(2)-Cl(2)	79.79(4)
Cl(2)-Mo(1)-Cl(3)	141.74(5)	N(1)-Mo(2)-N(2)	74.45(13)
Cl(1)-Mo(1)-Cl(3)	85.18(5)	N(1)-Mo(2)-Cl(1)	135.43(12)
Cl(2)-Mo(1)-Cl(4)	86.12(5)	N(1)-Mo(2)-Cl(2)	87.35(12)
Cl(1)-Mo(1)-Cl(4)	140.29(5)	N(2)-Mo(2)-Cl(1)	84.15(13)
Cl(3)-Mo(1)-Cl(4)	83.63(4)	N(2)-Mo(2)-Cl(2)	133.63(12)
Cl(3)-Mo(1)-Mo(2)	93.50(4)	N(1)-Mo(2)-Mo(1)	88.80(12)
Cl(4)-Mo(1)-Mo(2)	92.55(4)	N(2)-Mo(2)-Mo(1)	86.47(12)
Mo(1)-Cl(1)-Mo(2)	79.05(4)	Mo(1)-Cl(2)-Mo(2)	79.57(5)

^aCNT = cyclopentadienyl ring centroid.

Captions for Figures

Figure 1. ORTEP view of the $\text{CpMoCl}_2(\mu\text{-Cl})_2\text{Mo}(\text{as-ox})\text{Cp}$ molecule. Ellipsoids are drawn at the 50% probability level. The H atoms are omitted for clarity.

Figure 2. \overline{M}_n (squares) and PDI (triangles) as a function of conversion for the PS obtained in toluene (30% v/v) at 90°C in the presence of: (a) $\text{CpMoCl}_2(\mathbf{R}^*\mathbf{2dad})/\text{Al}(\text{O}^i\text{Pr})_3$ (S/Mo/IEA/Al = 173/1/1/1); (b) $\text{Cp}_2\text{Mo}_2\text{Cl}_4(\text{as-ox})$ (S/Mo/BEB = 453/1/1.6). In both graphs, the straight line corresponds to the theoretical \overline{M}_n for $f = 0.6$.

Figure 3. First order kinetics for the monomer consumption in the ATRP of styrene catalyzed by the systems $\text{CpMoCl}_2(\mathbf{R}^*\mathbf{2dad})/\text{Al}(\text{O}^i\text{Pr})_3$ (squares) and $\text{Cp}_2\text{Mo}_2\text{Cl}_4(\text{as-ox})$ (circles).

Figure 1

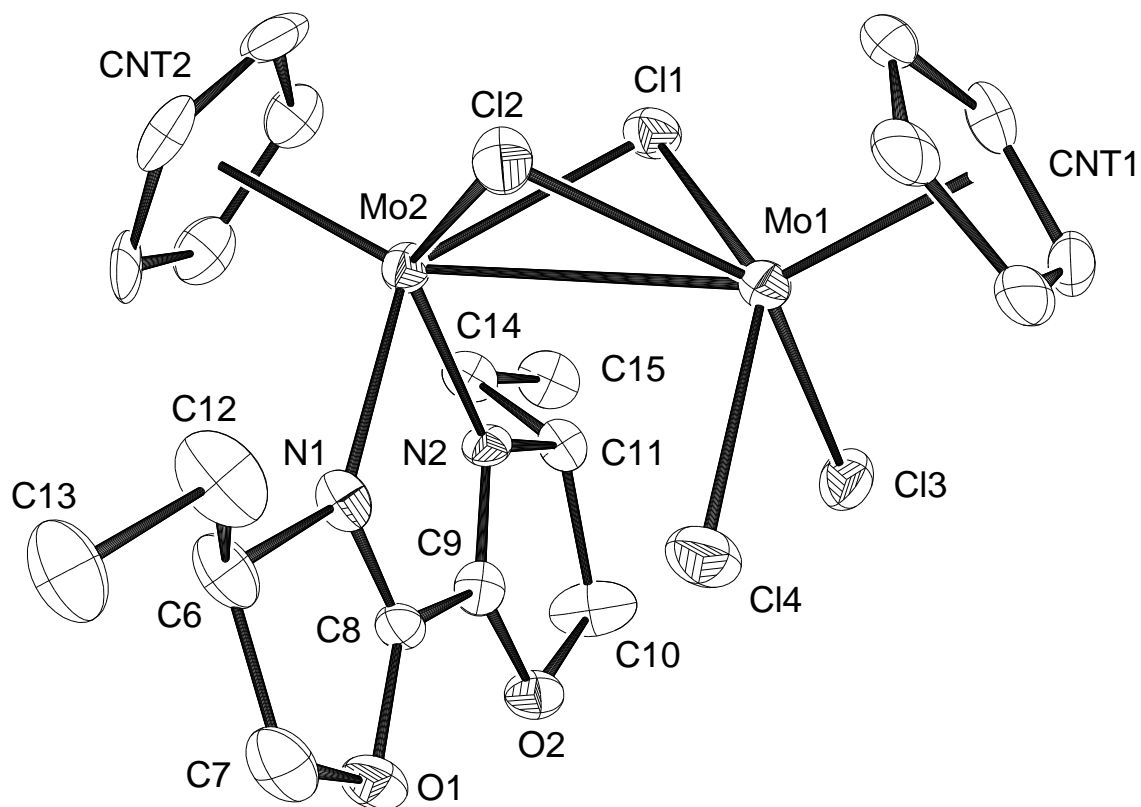


Figure 2

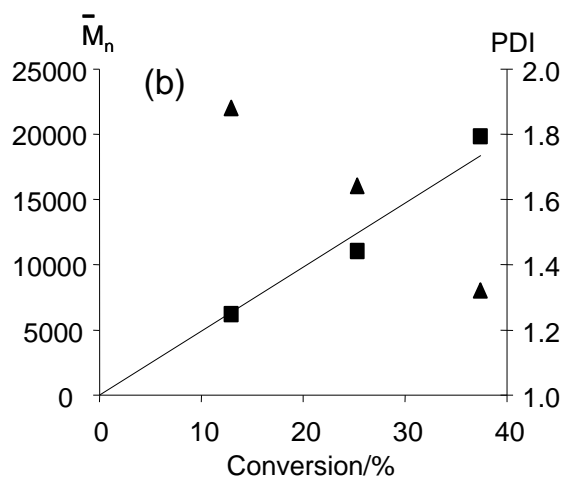
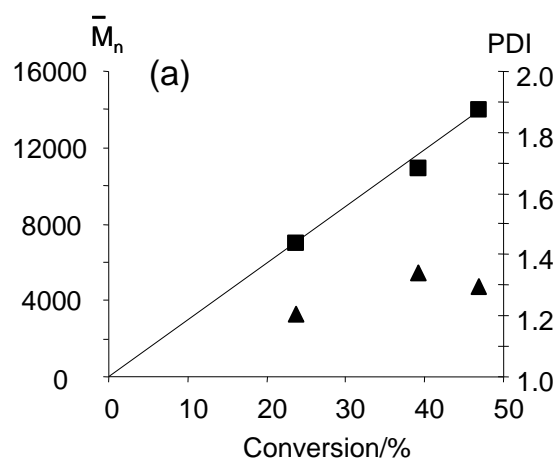
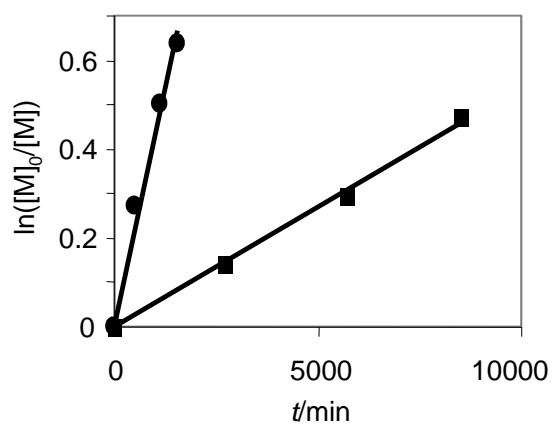
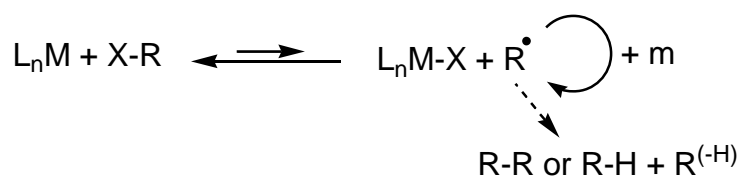


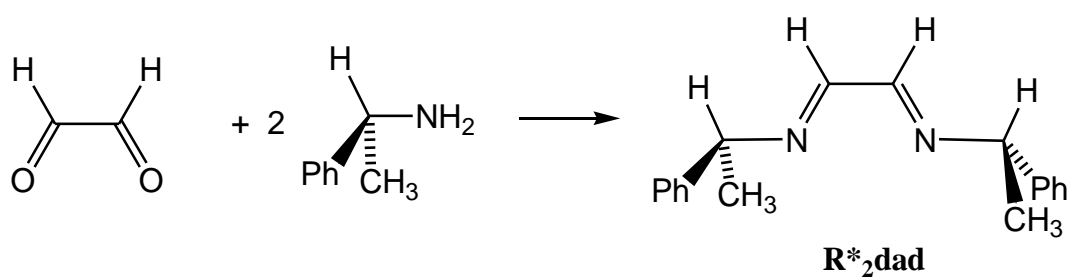
Figure 3



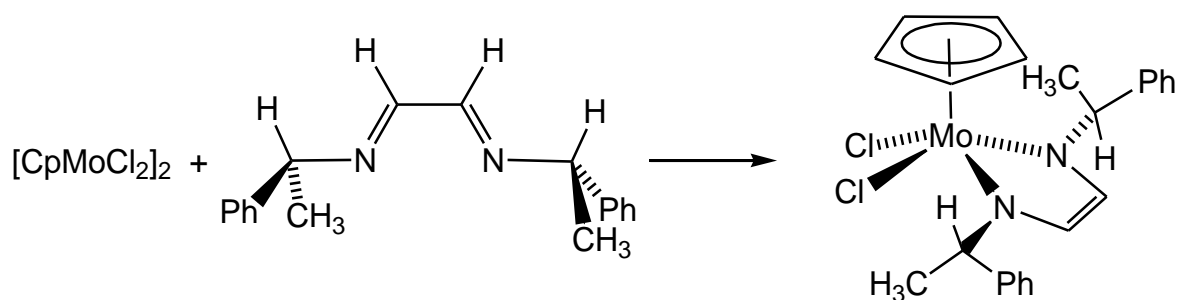
Scheme 1



Scheme 2



Scheme 3



Scheme 4

